ACS APPLIED MATERIALS & INTERFACES

Article

Fabrication of Crack-free Photonic Crystal Films on Superhydrophobic Nanopin Surface

Tian Xia, Wenhao Luo, Fan Hu, Wu Qiu, Zhisen Zhang, Youhui Lin, and Xiang Yang Liu

ACS Appl. Mater. Interfaces, **Just Accepted Manuscript** • DOI: 10.1021/acsami.7b04653 • Publication Date (Web): 08 Jun 2017

ACS Publications

ACS Applied Materials & Interfaces is published by the American Chemical Society. 1155 Sixteenth Street N.W., Washington, DC 20036

Fabrication of Crack-free Photonic Crystal Films on Superhydrophobic Nanopin Surface

Tian Xia, [†] *Wenhao Luo,* [†] *Fan Hu,* [†] *Wu Qiu,* [†] *Zhisen Zhang,* [†] *Youhui Lin,* [†, §, ⊥, *] *and Xiang Yang Liu* [†, ‡, *]

[†] Research Institute for Biomimetics and Soft Matter, Fujian Provincial Key Laboratory for Soft Functional Materials Research, College of Materials & College of Physical Science and Technology, Xiamen University, Xiamen 361005, China. Email: linyouhui@xmu.edu.cn or phyliuxy@nus.edu.sg

[‡] Department of Physics, National University of Singapore, 2 Science Drive 3, Singapore, 117542, Singapore

[§]Institute of Nanotechnology, Karlsruhe Institute of Technology, 76344 Eggenstein-Leopoldshafen, Germany

[⊥]Institute of Applied Physics, Karlsruhe Institute of Technology, 76128 Karlsruhe, Germany

KEYWORDS: Superhydrophobic Surface, Photonic Crystal, Nanostructure, Crack-free, soft assembly

ABSTRACT: Based on their superior optical performance, photonic crystals (PCs) have been investigated as excellent candidates for widespread applications including sensors, displays, separation processes, and catalysis. However, fabrication of large-area PC assemblies with no defects and structurally controllable is still a tough task. Herein, we develop an effective strategy for preparing centimeter-scale crack-free photonic crystals films by the combined effects of soft assembly and superhydrophobic nanopin surfaces. Owing to its large contact angle and low adhesive force on the superhydrophobic substrate, the colloidal suspension exhibits a continuous retraction of the three-phase (gas−liquid−solid) contact line (TCL) in the process of solvent (water molecules) evaporation. The constantly receding TCL can bring the colloidal spheres closer to each other, which could timely close the gaps due to the loss of water molecules. As a result, close-packed and well-ordered assembly structures can be easily obtained. We expect that this work may pave the way to utilize novel superhydrophobic materials for designing and developing high-quality PCs and to apply PCs in different fields.

INTRODUCTION

Recently, photonic crystals (PCs) have attracted tremendous interests for controlling the flow of light with periodic structure.[1-6] Due to their unique features, PCs hold great promise for a wide range of applications including sensors,[7-10] solar cells,[11] displays,[2] and optical devices.[12-13] However, owing to the unavoidable shrinkage of the colloidal particles and tensile stress generated in the process of their assembly, cracks are spontaneously produced and often inevitable during the formation of PCs films, which greatly degrade their optic quality and strength.[4, 14] Therefore, it is highly desired to fabricate large-scale self-assembled structures with no defects and structurally controllable.[14]

On the other hand, superhydrophobic surfaces, which possess water contact angles larger than 150° and their roll-off angles lower than 5°, have also aroused considerable attention over the past several decades for their attractive performances in colloidal assembly, water repellency, self-cleaning and anti-fog.[4, 15-16] Up to now, numerous approaches have been proposed to construct superhydrophobic surfaces.[17, 18] Generally, fabrication of the rough surface and subsequently coating the as-prepared surface using low surface energy materials (e.g., fluorine-containing material) are two necessary processes in preparing superhydrophobic surfaces.[14] Rough surfaces can trap air component in such fractal structures. Since air component has a water contact angle of 180°, such component can causes an increase in the total contact angle according to Cassie's law.[19]

$$\cos\theta_c = f_1 \cos\theta_1 + f_2 \cos\theta_2 \qquad (1)$$

θ_c is the total contact angle of flat film; θ_1 and θ_2 represent the contact angles of two different components; and f_1 and f_2 are their corresponding fractions of surface area. Here, component 2 is

set to the air component. It means that materials with smaller f_1 and larger θ_1 will make substrates more hydrophobic. As a result, rough micro- and nanostructures with small f_1 have been widely used to prepare superhydrophobic substrates.[18, 20] Unexpectedly, Song and Jiang et al. have recently revealed improved assembly structure of latex particles on certain superhydrophobic substrates.[4] Such pioneering study prompted researchers to evaluate whether other matrices will improve colloidal assembly and understand the role of superhydrophobic substrates. Here, we presented a simple strategy for the fabrication of centimeter-scale crack-free colloidal PCs films on superhydrophobic nanopin substrates.

RESULTS AND DISCUSSION

Synthesis and Characterizations of Superhydrophobic Nanopin Surface. The fundamental principle of constructing superhydrophobic nanopin substrates by the bottom-up process [18] is illustrated in Figure 1A. Such approach avoids complicated synthesis, special equipment as well as the addition of toxic reductants.[18] Firstly, $CoCl_2 \cdot 6H_2O$ and $CO(NH_2)_2$ were dissolved in water, and placed into sealed containers with glass substrates. Cleaned substrates are hydrophilic, with water contact angles of $20 \pm 5°$ (Figure S1). After 24 h incubation at 60 °C, the deposited films were washed with ethanol, and then characterized using field emission scanning electron microscope (FE-SEM). As seen in Figure 1B, a large number of scattered nano-needles with a cone-like morphology deposited onto the surface of glass. According to previous reports and our X-ray diffraction (XRD) result (Figure S2), cobalt hydroxide with brucite-type (BCH) was the main component of these needles.[21] At this step, the rough BCH nanopin films were still hydrophilic (Figure 1B). To obtain a surface with superhydrophobic properties, the rough surface must be further functionalized with low surface energy molecules.[18] Therefore, sodium laurate

molecules were used for subsequent coating lauric acid on BCH surfaces. After incubation, the lauric acid-coated BCH-LA films were washed thoroughly with ethanol and then dried at room temperature. It is difficult to distinguish between BCH and BCH-LA films according to their crystal structure and morphology (Figure 1B, 1C, and Figure S2). We can clearly see that shows that each top of these nano-needles is very sharp through transmission electron microscope (TEM) image (Figure 1D). The obtained needle morphology is suitable for constructing superhydrophobic surface based on Cassie's law.[18] Although it is difficult to distinguish between the BCH and BCH-LA using SEM and XRD, the conjugation of lauric acid onto the exposed cobalt hydroxide surface could be characterized by Fourier transform infrared (FTIR) spectroscopy and surface wettability. As shown in Figure 1E, FTIR spectra of lauric acid coated surface showed new peaks at around 2855 cm^{-1} (symmetric vibrations of $-CH_2-$ and $-CH_3-$ groups) and 2924 cm^{-1} (C-C asymmetric vibrations), which confirmed the attachment of lauric acid onto the BCH surface. Furthermore, the incubation of hydrophilic BCH films into sodium laurate solutions results in superhydrophobic surfaces, with water contact angles of $160 \pm 1°$ (Figure 1C). At the same time, the resulting superhydrophobic substrates have good stability, which could maintain for at least 1 month (Figure S3).

Fabrication of Well-ordered Photonic Crystal Film on Superhydrophobic Nanopin Surface. After successfully constructing superhydrophobic nanopin surfaces, we then address the possibility of applying such substrates into the preparation of crack-free PCs. In our experiments, Poly (styrene-methyl methacrylate-acrylic acid) latex nanospheres [P(St-MMA-AA)] with three different sizes (220 nm, 250 nm, 270 nm) were chosen as a building block model to form the quasi-amorphous photonic structures. It is believed that P(St-MMA-AA) nanoparticles possess core-shell structures, i.e., their hydrophobic polystyrene core is

encapsulated by a thin hydrophilic copolymer shell [P(MMA-*co*-AA)] with carboxyl groups (-COOH) attached to their surface (Figure S4).[22] Figure 2A-2D and Figure S5 show that SEM images of the P(St-MMA-AA)-based PCs prepared on hydrophilic and superhydrophobic substrates, respectively. We can see the obvious difference between the two types of samples at different scales. The colloidal PCs films with a large number of cracks on hydrophilic substrates were observed, whereas samples on superhydrophobic substrates were crack-free under the same conditions. Similarly, the significant difference for two samples could be readily distinguishable by atomic force microscopy (AFM). On hydrophilic substrates, there were many apparent defects such as dislocations, stacking faults and point defects (Figure 2E and Figure S6A). However, almost no crack occurred on superhydrophobic substrates (Figure 2F and Figure S6B). In addition, the Fourier format (FFT) image in the inset of Figure 2F further demonstrated well-ordered assembly structures of colloidal particles on superhydrophobic substrates.[4] Moreover, their difference can also be seen directly by naked eyes (Figure S7).

Red Shift Phenomenon of Reflection Peak Position of Photonic Crystal Film on Superhydrophobic Nanopin Surface. Another notable feature of as-obtained PCs on these two different surfaces is that the red shift of reflection peaks was observed for all samples on superhydrophobic substrates. In comparison with colloidal assembly on hydrophilic substrates, their characteristic peak positions on superhydrophobic substrates exhibited significant redshift (more than 8 nanomaters) (Figure 3A). In addition, control studies indicated that another poly (styrene-*co*-acrylic acid) colloidal spheres [P(St-AA)] could also have similar effect (Figure S8A). We can explain such "red shift" phenomenon observed on superhydrophobic substrates by Bragg's law[23]:

$$\lambda_{max} = 2d_{111}n_{\text{eff}}\sin\theta \qquad (2)$$

$$n_{\text{eff}}^2 = f n_0^2 + (1-f) n_c^2 \qquad (3)$$

$$d_{111} = \sqrt{2/3}\, D \qquad (4)$$

where λ_{max} is the wavelength for maximum reflection; d_{111} represents interplanar spacing, which is equal to $\sqrt{2/3}$D; n_{eff} represents the effective refractive index of the colloidal PCs; θ is an angle of incident light; n_0 and n_c represent the refractive index of the polystyrene and the air respectively; D represents the diameter of the colloidal spheres; f is the filling factor of the as-obtained PCs, which depends on the compactness of colloidal spheres arrangement. Since the parameters including D, n_0, n_c, and θ ($n_0 = 1.6$, $n_c = 1$, $\theta = 90°$) are constant in a given system, we obtain the relationship between λ_{max} and f:

$$\lambda_{max} = C_1\sqrt{C_2 f + C_3} \qquad (5)$$

Here, $C_1 = 2\sqrt{2/3}D\sin\theta$; $C_2 = n_0^2 - n_c^2$; $C_3 = n_c^2$. According to Equation 5, λ_{max} is considered to be proportional to the filling factor f as C_1 and C_2 are positive. Therefore, we reasoned that the redshift phenomenon might be because of a more close-packed structure of colloidal particles after self-assembled on the superhydrophobic substrate. That is to say that the value of f increases when the assembly structure are denser and thus leads to larger λ_{max}. The SEM data of colloidal particles assembled on hydrophilic and superhydrophobic substrates confirmed our hypothesis (Figure 3B, 3C, and Figure S8B, S8C). For instance, on superhydrophobic substrates, the average distance of 220 nm P(St-MMA-AA) between two beads was 22 nm shorter than that obtained on hydrophilic substrates (Figure 3B, 3C). Additionally, colloid assembly by using P(St-MMA-AA) spheres usually exhibited more closed-packed structures than P(St-AA) spheres, which was mainly because P(St-MMA-AA) spheres are softer than P(St-AA).

The Role of Superhydrophobic Nanopin Surface on Constructing Crack-free and Close-packed Photonic Crystal Film. To make clear the factors which influence colloidal arrangement, we investigated whether contact angles and adhesive forces could affect the morphologies and optical properties of PCs (Figure 4). Table S1 shows that the adhesive forces for the hydrophilic glass substrate (486.9±15.5 μN) and the superhydrophobic substrate (2.6±1.0 μN) are greatly different. For hydrophilic glass substrate, the adhesive forces between liquid molecules and substrate are stronger than the cohesive forces that result from the self-interaction of the liquid molecules. Whereas for superhydrophobic substrate, the solid/liquid interactions are weaken and owing to large contact angle, the liquid/liquid interactions are strengthen. As a result, two distinctly different modes of three-phase (gas −liquid− solid) contact line (TCL) were observed,[24] i.e., receding TCL for low-adhesive surface and pinned TCL for high-adhesive surface (Figure 4A, 4B). During drying process, the pinned TCL produced by high-adhesive substrate could not effectively release tensile stress. When the tensile stress was gradually accumulated until the critical stress was exceeded, the unavoidable cracks could be formed upon shrinkage of the colloidal spheres.[4] However, the constantly receding TCL on superhydrophobic substrates released the tensile stress in time, which could not reach the ultimate stress. Consequently, the vast majority of the cracks were eliminated. Taken together, the schematic representation of the self-assembly process of soft and flexible spheres on these two substrates is shown in Figure 5.

CONCLUSIONS

In summary, we demonstrated an interesting example that superhydrophobic nanopin surface could serve as an excellent substrate for preparing large-area crack-free PCs films. When the suspension of colloidal particles was self-assembled on a high-adhesive hydrophilic substrate,

colloidal spheres had a tendency to crack due to the loss of solvent (water) molecules. In contrast, when soft colloidal spheres were self-assembled on a superhydrophobic substrate with low adhesive, the constantly receding TCL could keep the free shrinkage of latex without limitation, which could close the gap in time. As a result, close-packed and well-ordered assembly structures could be easily obtained. Additionally, the homogeneity and monodisperesability of colloidal particles may also influence colloidal assembly. We visualize that more perfectly ordered PCs will be developed by using excellent quality of pristine nanoparticles and suitable superhydrophobic surfaces in the future. This work may pave the way to utilize novel superhydrophobic materials for designing and developing high-quality PCs and to apply PCs into optical devices, catalysis, and sensors.

MATERIALS AND METHODS

Materials. Acrylic acid (AA), methyl methacrylate (MMA) and styrene (St) were obtained from XiLong Scientific Co., Ltd., China. Cobalt chloride hexahydrate, urea and ammonium persulfate (APS), were purchased from Sinopharm Chemical Reagent Co., Ltd. (SCRC), China. Sodium laurate (Mw = 222.30 g/mol) was gained from Aladdin Reagent Inc., Shanghai, China. All other chemicals used are analytical reagent grade. Ultrapure water prepared from a Millipore water purification system (18.2MU, Milli-Q; Millpore Co., USA) was used in the whole the experiment.

Measurements and characterizations. SEM images for different substrates and the PCs were recorded by using a field emission scanning electron microscope (SU-70, Hitachi, Japan) operating at 5 kV after sputtering a thin layer of platinum onto the samples. The morphology and average size of the colloidal spheres were carried out by using nano measurer 1.2 analyzing

Software. Atomic force microscope (AFM) images of as-prepared samples were determined using an atomic force microscope (Bruker Dimension Icon). Optical properties of the particles were recorded by a fiber-optic spectrometer (USB2000+, Ocean Optics) to detect the reflection spectra. Photographs of the structural colors on surfaces were taken using a digital camera (EOS 700D, Canon, Japan) with a micro lens (MACRO 100mm). The crystal structures of BCH and BCH-LA films were evaluated by X-ray diffraction (XRD, Bruker D8). The FT-IR spectra of BCH and BCH-LA films was evaluated by microscopic infrared spectrometer (Nicolet IN10, Thermo Fisher Scientific). Transmission electron microscopy (TEM) images of the BCH films were recorded by a transmission electron microscope (JEOL JEM-2100). The water contact angles on different substrates were recorded using a Dataphysics DSA100 contact-angle system at room temperature. The adhesive forces measurements were performed with a microelectromechanical balance system (DCAT 11, Dataphysics). A drop of ultrapure water (3 μL) was added to a metal ring. After then, such drop was controlled to extrude the substrate under a constant speed (0.004 $mm \cdot s^{-1}$) and allowed to relax. For each substrate, the adhesive force was measured 5 times in parallel.

Preparation of superhydrophobic nanopin substrates. Superhydrophobic nanopin substrates synthesized through a chemical-base deposition method.[18] Briefly, 1.607 g $CoCl_2 \cdot 6H_2O$ and 9 g $CO(NH_2)_2$ were firstly dissolved in 45mL ultrapure water. Next, 5 mL beaker used as a deposition substrate was put into sealed container filled with above aqueous solution, and kept in a drying oven at 60 °C for 24 h. We note that all substrates were sonicated in lye for 30 min and rinsed with a large amount of ultrapure water before use. The obtained rough BCH surfaces were then collected, washed thoroughly with ethanol and allowed to dry under room temperature. Following the deposition, the resulting rough BCH films were further

modified by the addition of 0.1 M sodium laurate molecules. The above mixture was kept at 60 °C for 5 h in sealed container, and then the BCH-LA films were obtained after being rinsed by ethanol and dried. The contact angle can be varied by adjusting the concentration of sodium dodecanoate aqueous solution.

Synthesis of different latex nanoparticles. The latex particles of poly (St-MMA-AA) were prepared by a direct one-step emulsion polymerization technique.[22, 25] In a typical process, MMA (1.06 mL), St (22 mL) and AA (0.925 mL) were dispersed in ultrapure water (100 mL). And then, the emulsifier sodium dodecyl benzene sulfonate (SDBS) with an appropriate amount (0–0.004 g, below the critical micelle concentration) was dissolved into above solution. The latex particles with different sizes could be prepared by tuning the concentrations of SDBS. Another 15 mL of 0.14 M ammonium persulfate aqueous solution was added to the above mixture, and was kept at 80 °C for 10 h with continuous stirring under confined and nitrogen conditions. For the monodispersed colloidal nanoparticles of poly (St-AA), they were synthesized through soap-free emulsion polymerization. Briefly, St (38.5 mL), AA (0.3334 mL) and ultrapure water (300 mL) were dispersed in 500 mL four-necked flask in which was mixed for 0.5 h under confined and nitrogen conditions. Following the addition of 15 mL of ammonium persulfate (0.175 g) aqueous solution, the polymerization was continued at 70 °C for 7 h under continuous stirring. Finally, the resulting colloidal nanoparticles were collected after centrifuging.

Construction of Colloidal Crystal Films. The thin films of photonic crystals were prepared by gravity deposition method. Prior to use, the poly (St-MMA-AA) and poly (St-AA) suspension were sonicated for 15 min to disperse any particle aggregates. By adding the 20 wt% colloidal particles suspension (1 g) into the 5 mL BCH-LA beaker, the films with large-scale and crack-free structure can be obtained after drying at room temperature.

ASSOCIATED CONTENT

Supporting Information

This material is available free of charge via the Internet at http://pubs.acs.org.

SEM images, water contact angles, X-ray pattern, superhydrophobic stability, 3D AFM images, UV−vis reflection spectra, visual color images, and adhesive forces of different substrates.

AUTHOR INFORMATION

Corresponding Author

*E-mail: linyouhui@xmu.edu.cn or phyliuxy@nus.edu.sg

Notes

The authors declare no competing financial interest.

ACKNOWLEDGMENT

This work is financially supported by National Nature Science Foundation (Nos. 21401154, U1405226), 111 project (B16029), Guangdong Natural Science Foundation (2014A030310005), the Fundamental Research Funds for the Central Universities of China (Nos. 20720170011, 20720140528), Ph.D. Programs Foundation of Ministry of Education of China (20130121110018), Fujian Provincial Department of Science & Technology (2014H6022). X.Y.L.'s primary affiliation is the Department of Physics, National University of Singapore.

ABBREVIATIONS

Photonic crystal, PC; field-emission scanning electron microscope, FE-SEM; X-ray diffraction, XRD; brucite-type cobalt hydroxide, BCH; lauric-acid-coated cobalt hydroxide, BCH-LA; transmission electron microscope, TEM; fourier transform infrared spectroscopy, FTIR; fourier format, FFT; Poly (styrene-methyl methacrylate-acrylic acid), P(St-MMA-AA); atomic force microscopy, AFM; poly (styrene-*co*-acrylic acid), P(St-AA); three-phase contact line, TCL.

REFERENCES

1. Kuang, M.; Wang, J.; Jiang, L., Bio-inspired Photonic Crystals with Superwettability. *Chem. Soc. Rev.,* **2016,** *45* (24), 6833-6854.

2. Zhao, Y.; Shang, L.; Cheng, Y.; Gu, Z., Spherical Colloidal Photonic Crystals. *Acc. Chem. Res.* **2014,** *47* (12), 3632-3642.

3. von Freymann, G.; Kitaev, V.; Lotsch, B. V.; Ozin, G. A., Bottom-up Assembly of Photonic Crystals. *Chem. Soc. Rev.,* **2013,** *42* (7), 2528-2554.

4. Huang, Y.; Zhou, J.; Su, B.; Shi, L.; Wang, J.; Chen, S.; Wang, L.; Zi, J.; Song, Y.; Jiang, L., Colloidal Photonic Crystals with Narrow Stopbands Assembled from Low-Adhesive Superhydrophobic Substrates. *J. Am. Chem. Soc.,* **2012,** *134* (41), 17053-17058.

5. Ge, J.; Yin, Y., Responsive Photonic Crystals. *Angew. Chem. Int. Ed.,* **2011,** *50* (7), 1492-1522.

6. Diao, Y. Y.; Liu, X. Y., Controlled Colloidal Assembly: Experimental Modeling of General Crystallization and Biomimicking of Structural Color. *Adv. Funct. Mater.,* **2012,** *22* (7), 1354-1375.

7. Hou, J.; Zhang, H.; Yang, Q.; Li, M.; Song, Y.; Jiang, L., Bio-Inspired Photonic-Crystal Microchip for Fluorescent Ultratrace Detection. *Angew. Chem. Int. Ed.,* **2014,** *53* (23), 5791-5795.

8. Ye, B.; Rong, F.; Gu, H.; Xie, Z.; Cheng, Y.; Zhao, Y.; Gu, Z., Bioinspired Angle-independent Photonic Crystal Colorimetric Sensing. *Chem. Commun.,* **2013,** *49* (46), 5331-5333.

9. Exner, A. T.; Pavlichenko, I.; Lotsch, B. V.; Scarpa, G.; Lugli, P., Low-Cost Thermo-Optic Imaging Sensors: A Detection Principle Based on Tunable One-Dimensional Photonic Crystals. *ACS Appl. Mater. Interfaces,* **2013,** *5* (5), 1575-1582.

10. Fei, X.; Lu, T.; Ma, J.; Wang, W.; Zhu, S.; Zhang, D., Bioinspired Polymeric Photonic Crystals for High Cycling pH-Sensing Performance. *ACS Appl. Mater. Interfaces,***2016,** *8* (40), 27091-27098.

11. Guldin, S.; Hüttner, S.; Kolle, M.; Welland, M. E.; Müller-Buschbaum, P.; Friend, R. H.; Steiner, U.; Tétreault, N., Dye-Sensitized Solar Cell Based on a Three-Dimensional Photonic Crystal. *Nano Lett.,* **2010,** *10* (7), 2303-2309.

12. Vlasov, Y. A.; Bo, X.-Z.; Sturm, J. C.; Norris, D. J., On-chip Natural Assembly of Silicon Photonic Bandgap Crystals. *Nature* **2001,** *414* (6861), 289-293.

13. Ryu, S. H.; Gim, M.-J.; Lee, W.; Choi, S.-W.; Yoon, D. K., Switchable Photonic Crystals Using One-Dimensional Confined Liquid Crystals for Photonic Device Application. *ACS Appl. Mater. Interfaces,* **2017,** *9* (3), 3186-3191.

14. Zhang, Z.; Shen, W.; Ye, C.; Luo, Y.; Li, S.; Li, M.; Xu, C.; Song, Y., Large-area, Crack-free Polysilazane-based Photonic Crystals. *J. Mater. Chem.,* **2012,** *22* (12), 5300-5303.

15. Wang, S.; Liu, K.; Yao, X.; Jiang, L., Bioinspired Surfaces with Superwettability: New Insight on Theory, Design, and Applications. *Chem. Rev.,* **2015,** *115* (16), 8230-8293.

16. Cao, M.; Guo, D.; Yu, C.; Li, K.; Liu, M.; Jiang, L., Water-Repellent Properties of Superhydrophobic and Lubricant-Infused "Slippery" Surfaces: A Brief Study on the Functions and Applications. *ACS Appl. Mater. Interfaces,* **2016,** *8* (6), 3615-3623.

17. Li, X.-M.; Reinhoudt, D.; Crego-Calama, M., What Do We Beed for a Superhydrophobic Surface? A Review on the Recent Progress in the Preparation of SuperhydrophobicSurfaces. *Chem. Soc. Rev.,* **2007,** *36* (8), 1350-1368.

18. Hosono, E.; Fujihara, S.; Honma, I.; Zhou, H., Superhydrophobic Perpendicular Nanopin Film by the Bottom-Up Process. *J. Am. Chem. Soc.,* **2005,** *127* (39), 13458-13459.

19. Cassie, A. B. D.; Baxter, S., Wettability of Porous Surfaces. *Trans. Faraday Soc.,* **1944,** *40*, 546-551.

20. Shiu, J.-Y.; Kuo, C.-W.; Chen, P.; Mou, C.-Y., Fabrication of Tunable Superhydrophobic Surfaces by Nanosphere Lithography. *Chem. Mater.,* **2004,** *16* (4), 561-564.

21. Hosono, E.; Fujihara, S.; Honma, I.; Zhou, H., Fabrication of Morphology and Crystal Structure Controlled nanorod and Nanosheet Cobalt Hydroxide based on the Difference of Oxygen-Solubility between Water and Methanol, and Conversion into Co3O4. *J. Mater. Chem.,* **2005,** *15* (19), 1938-1945.

22. Kong, X. Z.; Ruckenstein, E., Core–shell Latex Particles Consisting of Polysiloxane–poly(styrene-methyl methacrylate-acrylic acid): Preparation and Pore Generation. *J. Appl. Polym. Sci.,* **1999,** *73* (11), 2235-2245.

23. Busch, K.; John, S., Photonic Band Gap Formation in Certain Self-organizing Systems. *Phys. Rev. E.,* **1998,** *58* (3), 3896-3908.

24. Deegan, R. D.; Bakajin, O.; Dupont, T. F.; Huber, G.; Nagel, S. R.; Witten, T. A., Capillary Flow as the Cause of Ring Stains from Dried Liquid Drops. *Nature* **1997,** *389* (6653), 827-829.

25. Wang, J.; Wen, Y.; Feng, X.; Song, Y.; Jiang, L., Control over the Wettability of Colloidal Crystal Films by Assembly Temperature. *Macromol. Rapid Commun.,* **2006,** *27* (3), 188-192.

Table Of Contents (TOC) graphic

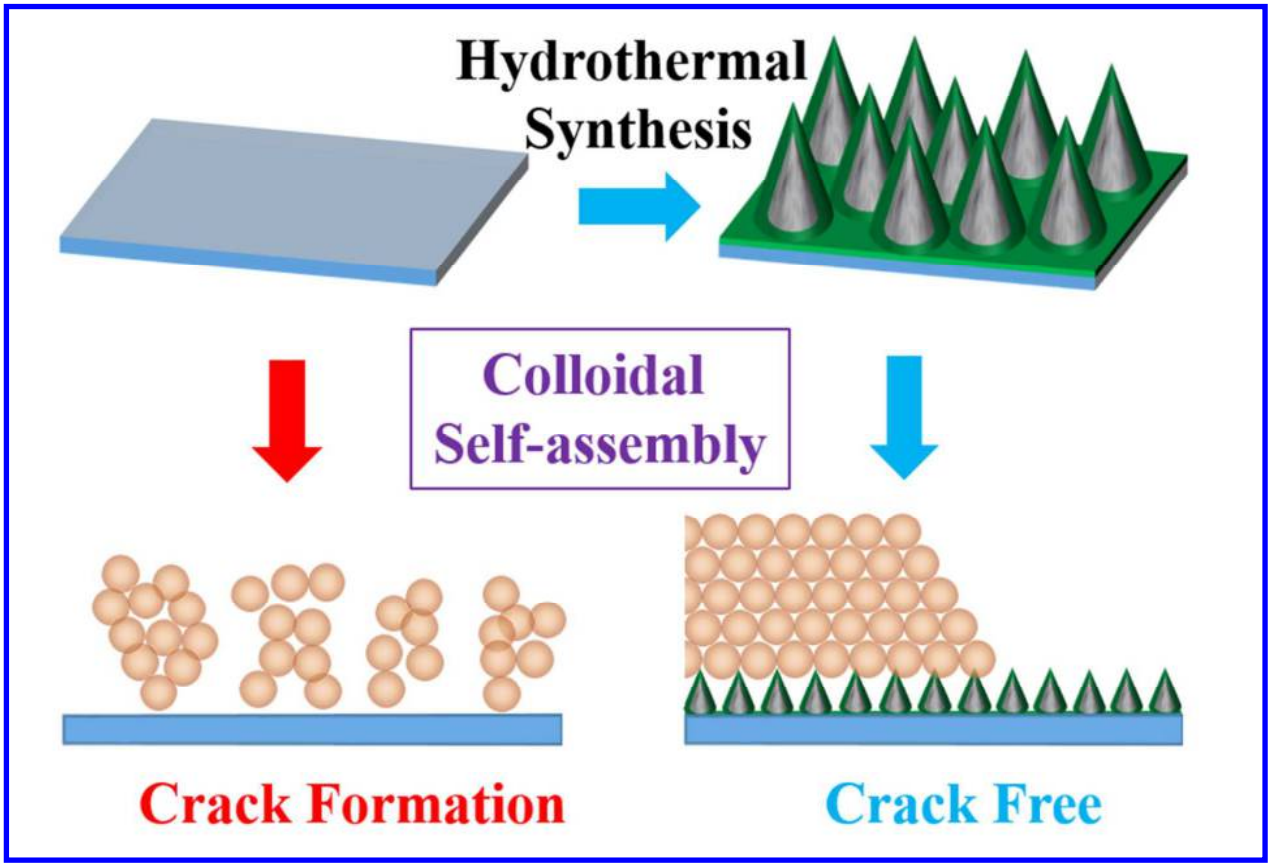

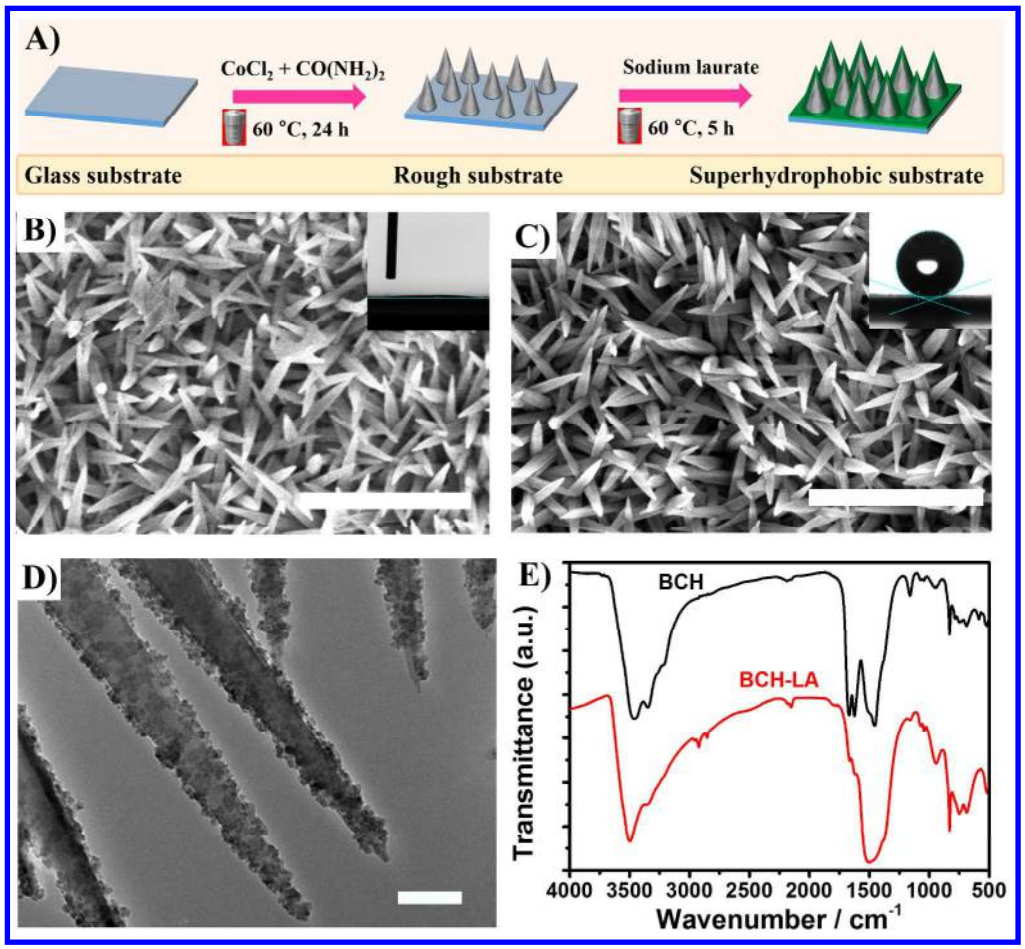

Figure 1. A) The fundamental principle for constructing superhydrophobic nanopin surface. B, C) SEM images of BCH and BCH-LA films and photographs of a water droplet on the corresponding surfaces (insets). The scale bars for SEM images are 3 μm. The insets indicate that rough BCH substrate is hydrophilic with contact angles of 0°, and BCH-LA substrate is superhydrophobic with contact angles of 160°±1°. D) TEM image of BCH-LA substrate. The scale bar is 100 nm. E) FT-IR spectra of BCH and BCH-LA films.

640x591mm (96 x 96 DPI)

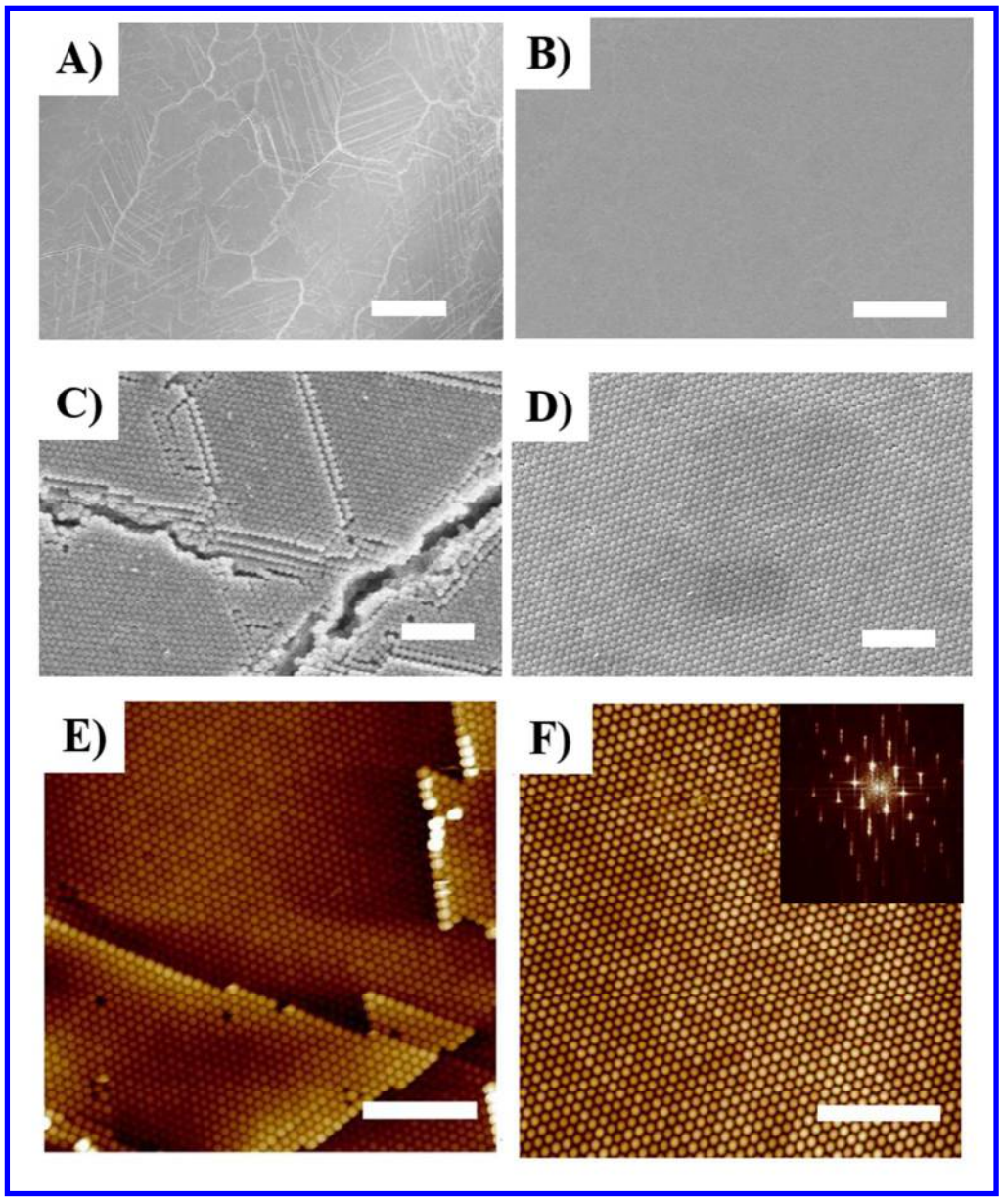

Figure 2. A-D) SEM images of as-prepared P(St-MMA-AA) colloidal particles with diameter of 220 nm assembled on hydrophilic (A, C) and superhydrophobic substrates (B, D) at different scales. The scale bars are 50 μm (A, B) and 3 μm (C, D), respectively. E, F) AFM images of the 220 nm P(St-MMA-AA) colloidal particles assembled on hydrophilic and superhydrophobic substrates. Inset in Figure D is an FFT image obtained from a large-area AFM image. The scale bars are 2.5 μm.

214x257mm (96 x 96 DPI)

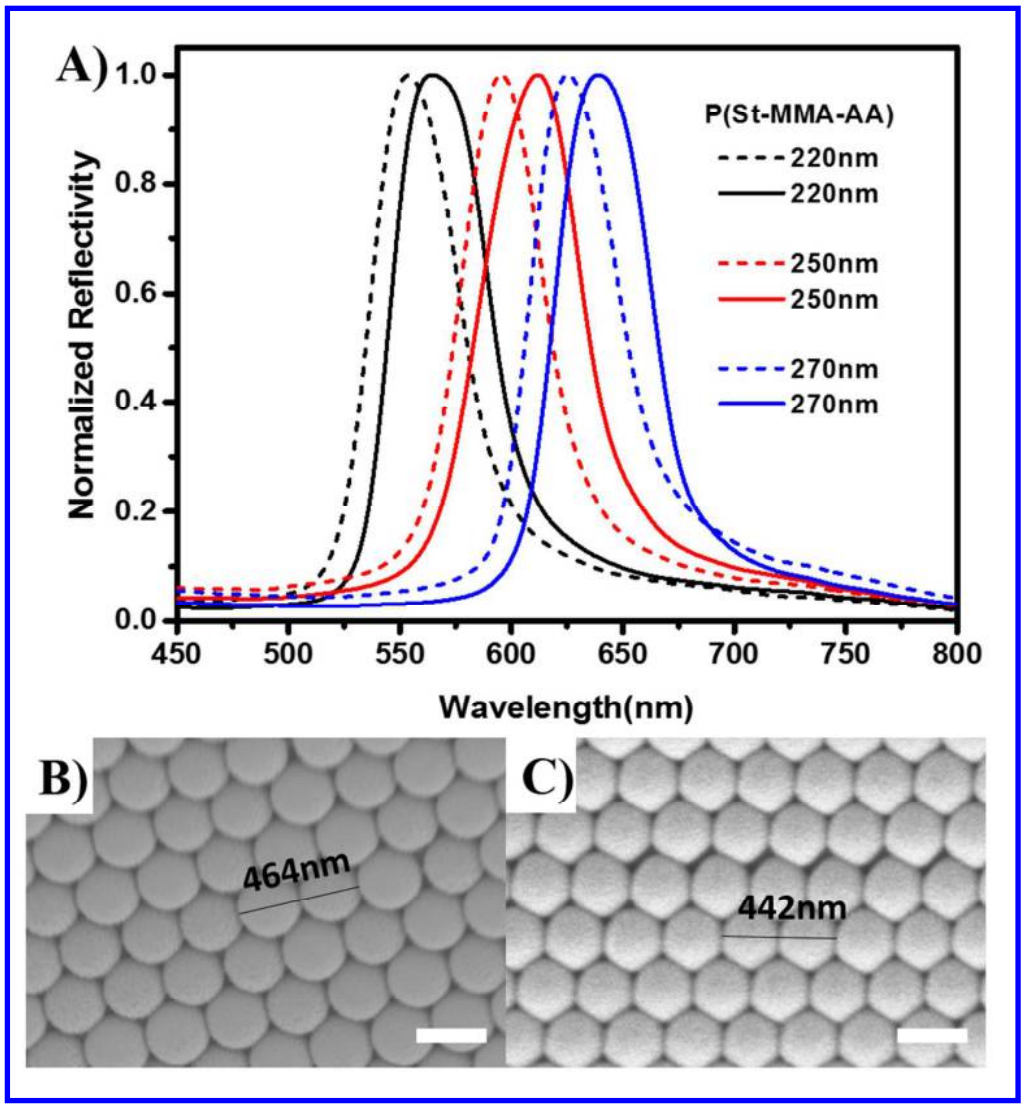

Figure 3. A) Normalized UV−vis reflection spectra of different diameters of P(St-MMA-AA) colloidal nanoparticles assembled on hydrophilic substrates (dotted line) and superhydrophobic substrates (solid line). B, C) SEM images of 220 nm P(St-MMA-AA) colloidal particles assembled on hydrophilic and superhydrophobic substrates, exhibiting more close-packed assembly structure on the superhydrophobic substrate. The scale bars are 250 nm. The total number of nanoparticles counted for average length of two beads was 20.

260x281mm (96 x 96 DPI)

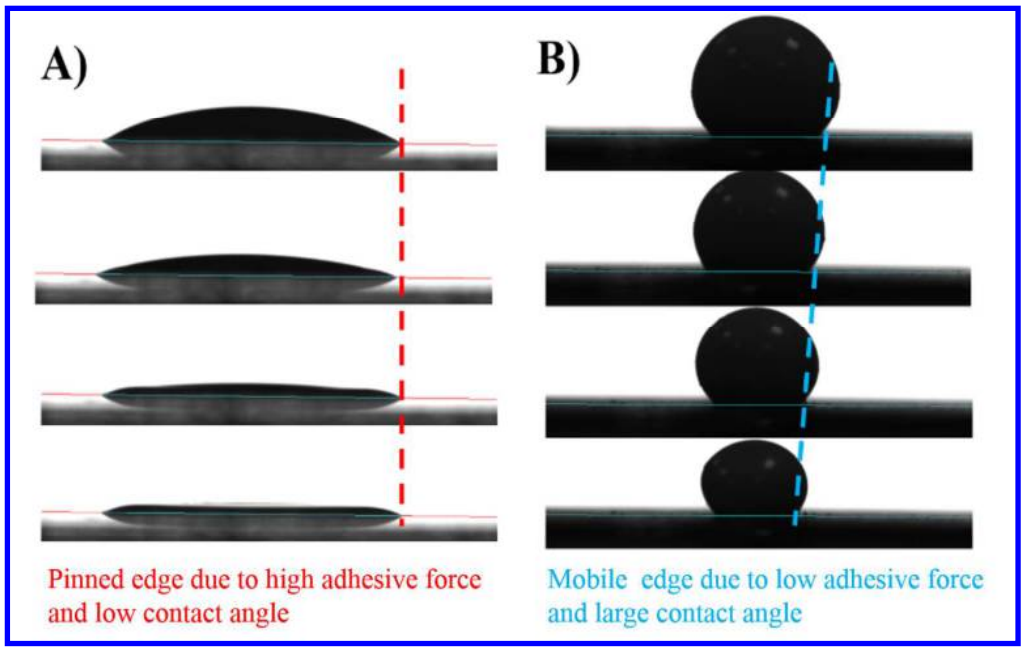

Figure 4. Photographs captured during the drying process of colloidal drops on high-adhesive hydrophilic substrate (A) and low-adhesive superhydrophobic substrate (B). The red dashed line displays the pinned TCL, and the blue dashed line represents the receding TCL.

399x250mm (96 x 96 DPI)

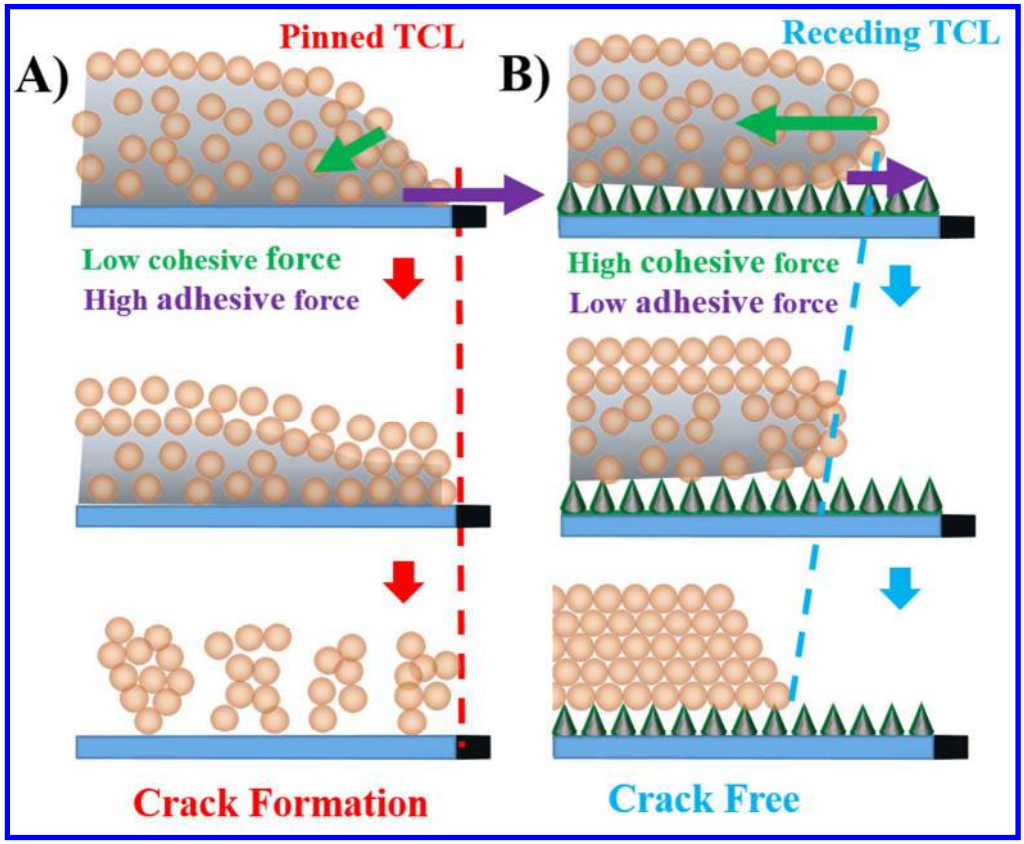

Figure 5. Schematic representation of colloidal nanoparticles assembled on the hydrophilic substrate (A) and superhydrophobic nanopin substrate (B).

250x206mm (96 x 96 DPI)